CHAPTER 4

DOSIMETRIC COMPARISON OF DIFFERENT PLANNING TECHNIQUES BASED ON FFF BEAM FOR LUNG SBRT

This chapter deals with the dosimetric comparison and evaluation of flattening filter-free (FFF) photon beam-based three-dimensional conformal radiotherapy (3DCRT), intensity-modulated radiation therapy (IMRT), and volumetric modulated arc therapy (VMAT) for lung stereotactic body radiotherapy (SBRT). RANDO phantom computed tomography (CT) images were used for treatment planning. The planning target volumes (PTVs) were determined by adding a 5 mm margin to the GTV. 3DCRT, IMRT, and VMAT plans were generated using a 6-MV FFF photon beam. Dose calculations for all plans were performed using the anisotropic analytical algorithm (AAA) and Acuros XB algorithms. The accuracy of the algorithms was validated using the dose measured in a CIRS thorax phantom. An introduction to the topic, a description of the methodology employed in the measurements, the formulas used in the calculations, the findings, and conclusions are presented below.

4.1 INTRODUCTION

Stereotactic body radiotherapy (SBRT) is a highly conformal treatment delivery of large doses administered in a few or as a single fraction. It is primarily preferred for the treatment of small to moderate-sized tumors of the lung, liver, and head and neck cancers. SBRT fractionation provides excellent results as an alternative to conventional treatment (Sebastian et al., 2018). Previous clinical studies have used three-dimensional (3D) conformal radiotherapy (3DCRT) or intensity-modulated radiation therapy (IMRT) more frequently for the treatment of lung SBRT (Cai et al., 2014; Visak et al., 2021). Recently, there has been an increased interest in treating these cases using volumetric modulated arc therapy (VMAT), also known as RapidArc (Varian Medical Systems, Inc., Palo Alto, CA, USA). It is an advanced technique capable of significantly accelerating dose delivery compared with those of 3DCRT and IMRT.

Conventionally, flattening filter (FF) photon beams are used in all of these treatment techniques. Recently, flattening filter-free (FFF) beams have been introduced as an additional option to FF beams. The main advantage of FFF beams compared with FF is a dose rate that is two to four times higher (Sharma 2011). The faster dose delivery of FFF beams can significantly reduce the lengthy treatment time of 3DCRT and IMRT, whereas the VMAT delivery time is mostly controlled by the

speed of gantry rotation, not by the dose rate. The rapid dose delivery in SBRT treatment reduces intra-fractional setup errors. The other advantages of the FFF beam over FF include a smaller penumbra, reduced head scatter, and higher dose per pulse (Dwivedi et al., 2021; Georg et al., 2011; Sahani et al., 2014). Therefore, FFF beams can lead to a more conformal dose distribution, reduced out-of-field dose, shorter treatment delivery time, and some gray radiobiological implications. The SBRT treatment requires faster treatment delivery and rapid dose fall off in the area surrounding the tumor (Vassiliev et al., 2009), which requires the use of FFF photon beams. Moreover, multiple studies on lung SBRT have been published that mostly focused on FF photon beams and actual patient CT datasets (Vassiliev et al., 2018; Xiao et al., 2009; Pokhrel et al., 2020; Ong et al., 2010; Verbakel et al., 2009; Wu et al., 2004; Hong et al., 2010). Therefore, in this study, we have opted a FFF beam rather than FF beam for lung SBRT in order to increase the available data on this topic. In addition to this, we have chosen an anthropomorphic phantom over real patient CT datasets because, firstly, this can allow for a highly consistent set of lung tumors, and secondly, this can facilitate dose measurements inside the phantom.

This study aimed to dosimetrically compare and evaluate the FFF photon beam-based 3DCRT, IMRT, and VMAT planning techniques for central and peripheral lung SBRT. In this study, we evaluated dosimetric indices, such as target dose conformity, dose fall-off outside the tumor, high-and low-dose spillage, dose homogeneity, doses to critical organs, and monitor units (MUs) for 3DCRT, IMRT, and VMAT SBRT plans based on FFF beams.

4.2 MATERIALS AND METHODS

4.2.1 RANDO phantom

The RANDO man phantom is an anthropomorphic phantom made of tissue-equivalent material embedded in a natural human skeleton, which has neither arms nor legs. Polyurethane was used to simulate the muscle and soft tissue. A material with the same effective atomic number as the soft tissue material and with a density almost three times lower was used to simulate the lungs. The phantom represents a male

body with a height of 175 cm and a weight of 73.5 kg. The RANDO man phantom was sliced at 2.5 cm intervals.

4.2.2 Tumor characteristics

Computed tomography (CT) images with a slice thickness of 1.5 mm of the RANDO man phantom were used for treatment planning. These images did not contain all of the organs. Therefore, the image registration of the RANDO phantom was performed using the CT images of an anonymous patient of similar height and weight. In this way, the soft tissue material of the RANDO phantom was substituted by the corresponding organ and contoured accordingly. An Eclipse treatment planning system (Eclipse TPS, Varian Medical Systems, Inc., Palo Alto, CA, USA) was used for image registration and contouring. A 3D model of the RANDO phantom is shown in Figure 4.1. The gross tumor volumes (GTVs) were delineated in two lung locations: central and peripheral. GTV was assigned a skeletal muscle material having a mass density of 1.05 g/cm^3 with a CT number of 48 HU to reproduce the effect of a lung tumor on the phantom (Suryanto et al., 2005). The planning target volume (PTV) was obtained by adding a margin of 5 mm to the GTV. A total of 24 PTVs, 12 per lung location, were delineated. These PTVs were a set of 12 distinct tumor sizes between 3.85 cc and 79.06 cc, with the same geometric center and with varying volumes. Both tumor locations were contoured with the same set of PTVs. The sizes of the 12 PTVs (n = 12) per location (central or peripheral) of the lungs are shown in Table 4.1.

4.2.3 Protocol for treatment planning

Treatment plans were evaluated using the Radiation Therapy Oncology Group (RTOG) protocols 0236, 0813, and 0915 (Xiao et al., 2009; Bezjak et al., 2019; Videtic et al., 2019). These protocols recommend the following: a minimum of seven static beams for 3DCRT, IMRT, and a 340° arc for VMAT planning; that the field apertures of each beam should shape the PTV with no additional margin, except for a small margin in the superoinferior direction if necessary; that treatment plans should be normalized to the beam isocenter (geometric center of the PTV); and that PTV coverage should be such that at least 95% of the PTV receives 100% of the prescribed

dose (60 Gy in three fractions). Treatment planning objectives and doses to organs at risk (OARs) were selected according to the aforementioned protocols.

4.2.4 Planning techniques

In this study, the 3DCRT, IMRT, and VMAT planning techniques for the SBRT of lung tumors were investigated. Treatment plans were generated using the Eclipse TPS (version 13.6). A 6-MV FFF photon beam from a True Beam linear accelerator (Varian Medical Systems, Inc., Palo Alto, CA, USA) was used for planning. Field apertures were created using a Millennium multileaf collimator (MLC) with 120 leaves. Radiation dose calculations for all of the plans were performed with a grid resolution of 2.5 mm using Acuros XB algorithm (dose-to-medium). All the plans were normalized such that the prescription dose covers 95% of the PTV. Plans were delivered at a dose rate of 1400 MU/min.

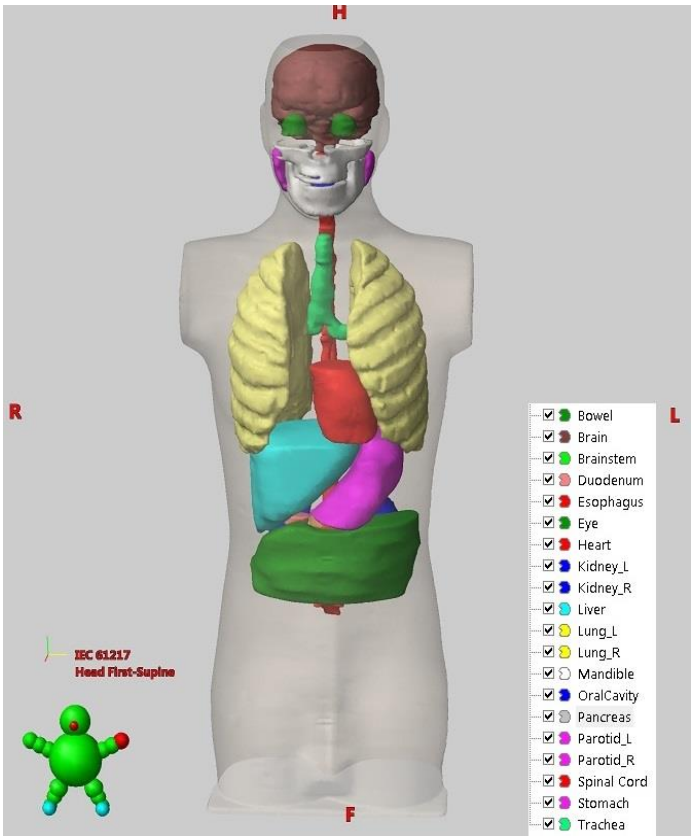

Figure 4.1 Three-dimentional (3D) model view of RANDO phantom; organs and tissues are represented by different colors.

Table 4.1 The size of the twelve PTVs (n = 12) per location (central or peripheral) of the lung used in this study.

PTV#	PTV Volume (cc)
1	3.85
2	7.78
3	13.6
4	19.62
5	27.86
6	32.32
7	40.34
8	45.95
9	55.97
10	61.79
11	71.53
12	79.06

PTV, planning target volume

4.2.4.1 FFF-VMAT

VMAT plans were generated using 6-MV FFF beams, consisting of two full coplanar arcs for centrally located targets and two ipsilateral arcs for the peripheral PTVs. Full arcs delivered the dose throughout a 358° gantry rotation, while the ipsilateral arcs covered 179°. Collimator rotations of 30° and 330° were used for the clockwise and counterclockwise arcs, respectively. It was used to minimize the tongue and groove effects of the MLC. The upper limit of the PTV dose in the optimization was set to a dose 15%–20% higher than the prescribed dose, while the lower limit was set at the prescription dose that covered 95% of the PTV. A relatively high weight was assigned to the lower limit of PTV compared to the upper limit. The VMAT plans were optimized with the photon optimization (PO) algorithm based on dose–volume objectives. The VMAT optimization process used the direct aperture optimization of volumetric doses. The PO algorithm optimizes gantry speed, MLC leaf sequence, and dose rate at each control point. This optimization process continued to the point where PTV achieved the desired dose, and manipulation of OAR constraints after that point can deteriorate the PTV coverage.

4.2.4.2 FFF-IMRT

We generated a non-coplanar IMRT plan using 6-MV FFF beams for each PTV. The plans consisted of 9 beams, of which 5 were non-coplanar. The beam angles were initially determined using the beam angle optimization algorithm (Varian Eclipse TPS 13.6) based on the location of the PTV and critical organs. IMRT planning was performed using these angles. Some beam directions were adjusted manually if the outcome of the optimized angles did not satisfy the dosimetric objectives. IMRT plans were generated using the same dose constraints as those employed for VMAT. The IMRT plans were iteratively optimized using PO algorithm to obtain a dose volume histogram (DVH), which met the dosimetric criteria established by RTOG. The MLC leaf sequences of each beam were dynamically generated using the sliding window technique.

4.2.4.3 FFF-3DCRT

The non-coplanar 3DCRT plans were generated using 6-MV FFF beams by maintaining the same beam angle arrangements defined for IMRT. The PTV size field apertures for each beam were created from the MLCs to achieve the highly conformal plan. The treatment plans were normalized to a point that closely corresponded to the geometric center of the PTV, which was also called the beam isocenter. The 3DCRT plans were manually optimized to meet target coverage and OAR-sparing objectives based on the RTOG protocols.

4.2.5 Plan evaluation

The plans were evaluated using the following dosimetric indices established primarily by the RTOG:

PTV coverage: This was defined such that at least 95% of the PTV received the prescribed dose and a minimum of 90% of the prescribed dose was delivered to 99% of the PTV.

Conformity index (CI): This was defined as the ratio of the volume receiving the prescribed dose (V_{PD}) to the volume of PTV receiving at least the prescribed dose (PTV_{PD}). This ratio was ideally planned to be less than 1.2, with an accepted minor deviation of up to 1.4.

$$CI = V_{PD}/PTV_{PD}. \quad (1)$$

High dose volume (HDV): The volume of tissue outside the PTV that received a dose greater than 105% of the prescribed dose was planned to be less than 15% of the PTV.

Low-dose location (D_{2cm}): The maximum dose to normal tissue located 2 cm from the PTV in all directions was evaluated.

Low dose volume ($R_{50\%}$): This was defined as the ratio of the volume receiving 50% of the prescribed dose (V_{50PD}) to the volume of the PTV.

$$R_{50\%} = V_{50PD}/PTV. \quad (2)$$

Dose limits to OARs: The bilateral lung volume receiving 20 Gy or more (V_{20}) was planned to be less than 10%. Maximum point doses to the spinal card dose, esophagus, and heart were also recorded for each plan. Dose constraints for OARs established by RTOG are shown in Table 4.2.

Table 4.2 RTOG dose constraints to OARs

Organ	Volume	Dose (Gy)
Lungs	10%	20
Spinal cord	Max point dose	18
Esophagus	Max point dose	27
Heart	Max point dose	30

Additionally, the plans were evaluated using the dosimetric indices established by other studies (ICRU 2010; Paddick et al., 2006).

Gradient index (GI): According to Paddick and Lippitz, GI is defined as the ratio of the volume receiving 50% of the prescribed dose (V_{50PD}) to the volume of prescription isodose (PIV).

$$GI = V_{50PD}/PIV. \quad (3)$$

Homogeneity index (HI): According to the International Commission on Radiation Units and Measurements 83, HI is defined as the ratio of the difference between the

near-maximum ($D_{2\%}$) and near-minimum ($D_{98\%}$) radiation dose in PTV volume to the median PTV dose ($D_{50\%}$).

$$HI = (D_{2\%}-D_{98\%})/D_{50\%}. \quad (4)$$

Maximum dose (D_{max}): The maximum point dose received by the PTV.

Monitor units (MUs): The total *MU* needed to deliver the prescribed dose of a treatment plan.

Beam on time (BOT): The duration of the time beam being used to deliver the planned *MUs*.

Treatment time (TT): The duration of treatment delivery for a treatment plan.

4.2.6 Statistical analysis

The SBRT plans generated by the three planning techniques were statistically compared. The statistical analysis between dosimetric indices of the plans was performed using a rank-based paired difference test (non-parametric Wilcoxon signed-rank test). This test was based on the probability (p) value if the calculated p-value was low ($p < 0.05$), the null hypothesis was rejected, and the difference between the two groups was considered significant. Therefore, it tested the null hypothesis for individual pairs of data columns.

4.2.7 Validation of dose calculation algorithms:

To validate dose calculation algorithms, such as Acuros XB and anisotropic analytical algorithm (AAA), treatment plans were created in a CIRS thorax phantom (model 002LFC; Computerized Imaging Reference Systems, Inc. [CIRS], Norfolk, VA, USA). The measurements were performed on a TrueBeam LINAC (Varian Medical Systems, Inc., Palo Alto, CA, USA) for a 6-MV FFF photon beam using a PinPoint ionization chamber (type 31016, PTW). To simulate central and peripheral lung tumors, the ion chamber was placed in the center of the left lung and the posterior periphery of the right lung. Three plans of each tumor location for fixed field sizes of 3 cm × 3 cm, 6 cm × 6 cm, and 10 cm × 10 cm were generated in eclipse TPS with nine fields spaced evenly in 40° gantry angle increments, starting at 0°, and each beam was set to 100 MU. The treatment dose of each plan was calculated using

Acuros XB (dose-to-medium [D_M]), Acuros XB (dose-to-water [D_W]), and AAA algorithms, and compared with the experimentally measured dose.

4.3 RESULTS

The statistics of dosimetric indices for all SBRT plans were obtained from the DVH analysis. Consequently, the plans for the three different techniques were compared using these indices. The results of the mean dosimetric indices for the FFF-3DCRT, FFF-IMRT, and FFF-VMAT treatment plans of the combined lung PTVs (all PTVs from central and peripheral lung locations) are summarized in Table 4.3. The same results according to the location of lung tumors (central and peripheral lung PTVs) are also evaluated separately in Tables 4. The dose distributions of the three different treatment techniques (FFF-3DCRT, FFF-IMRT, and FFF-VMAT) for PTV#8 (both central and peripheral) in the axial plane are shown in Figure 4.2. The mean DVH of the three different techniques for central and peripheral lung PTVs are illustrated in Figs. 4.3 and 4.4, respectively.

4.3.1 PTV Coverage

The FFF-3DCRT, FFF-IMRT, and FFF-VMAT plans of each PTV met the respective RTOG criteria for PTV coverage.

4.3.2 CI

Compared with FFF-3DCRT, the mean CI value improved with both FFF-VMAT and FFF-IMRT for combined lung PTVs, while the best CI was obtained with FFF-VMAT. Compared with central lung PTVs, peripheral lung PTVs achieved a better CI. All PTVs met the respective RTOG standards with three different techniques, excluding one smaller PTV located in the peripheral lung (PTV #1) and two smaller PTVs in the central lung (PTV #1 and PTV #2), which were planned using the FFF-3DCRT and showed minor deviations. Individual comparisons using the Wilcoxon test showed significant differences ($p < 0.05$) between the different techniques.

4.3.3 HDV and D_{2cm}

Similar to the CI, the mean values of HDV and D_{2cm} improved with FFF-VMAT and FFF-IMRT for combined lung PTVs. Central and peripheral lung PTVs

also showed a similar trend to combined lung PTVs, except for the FFF-IMRT, which showed improved D_{2cm} compared to FFF-VMAT for peripheral lung PTVs. Similar to CI, the Wilcoxon test for HDV and D_{2cm} indicated significant differences ($p < 0.05$) between different techniques, the difference being that the p-values for D_{2cm} between different techniques for peripheral lung PTVs did not show significant differences ($p > 0.05$).

4.3.4 $R_{50\%}$ and GI

Both $R_{50\%}$ and GI improved with FFF-3DCRT, the difference being $R_{50\%}$ for central lung PTVs that improved with FFF-VMAT. The Wilcoxon test for $R_{50\%}$ indicated significant differences ($p < 0.05$) between the different techniques, except that the p-values for $R_{50\%}$ between different techniques for central lung PTVs showed no significant difference ($p > 0.05$), and the $R_{50\%}$ between FFF-IMRT and FFF-VMAT plans for combined and peripheral lung PTVs being $p = 0.732$ and 0.417, respectively. The Wilcoxon test for GI between the different techniques also indicated significant differences ($p < 0.05$), except for the p-values for GI between FFF-3DCRT and FFF-IMRT plans for central lung PTVs, and between FFF-IMRT and FFF-VMAT plans for peripheral lung PTVs were $p = 0.427$ and 0.134, respectively.

4.3.5 HI, D_{max}, and $D_{2\%}$

The individual comparison (Wilcoxon test) for HI yielded significant differences ($p < 0.05$) between different techniques for both combined and peripheral lung PTVs, while for central lung PTVs, a significant difference in HI could not be established between different techniques ($p > 0.05$). Based on the Wilcoxon test for D_{max} and $D_{2\%}$, there was a significant difference ($p< 0.05$) between the different techniques, except for the p-value for D_{max} between the FFF-IMRT and FFF-VMAT plans for central lung PTVs being $p = 0.071$.

4.3.6 MUs, BOT, and TT

Compared with FFF-3DCRT, the mean MU values showed an increase of 34.28 % with FFF-IMRT, and 18.78 % with FFF-VMAT for combined lung tumors; 37.83 % with FFF-IMRT, and 23.08 % with FFF-VMAT for central lung tumors; and 30.01 % with FFF-IMRT, and 13.63 % with FFF-VMAT for peripheral lung tumors.

A similar increase in BOT was observed. Compared with the mean TT value of FFF-3DCRT, a drastic decrease in that of FFF-VMAT was observed in different lung sites, between 57.09 % and 60.39 %, while this increased between 10.78 % and 17.49 % in FFF-IMRT. The Wilcoxon test for MUs, BOT, and TT between the different techniques also indicated significant differences ($p < 0.05$).

4.3.7 Dose limits to OARs

All three treatment techniques met the OAR dose constraints. The Wilcoxon test for V_{20} and D_{max} (spinal cord, esophagus, and heart) showed significant differences between the different techniques ($p < 0.05$), except for the p-values for the following: D_{max} (spinal cord and esophagus) between FFF-3DCRT and FFF-IMRT ($p > 0.05$) for peripheral lung PTVs; D_{max} (esophagus) between FFF-3DCRT and FFF-IMRT for combined and central lung PTVs ($p > 0.05$); V_{20} (lung) between FFF-IMRT and FFF-VMAT for combined lung PTVs ($p > 0.05$); and V_{20} (lung) between FFF-3DCRT and FFF-VMAT for central lung PTVs ($p > 0.05$).

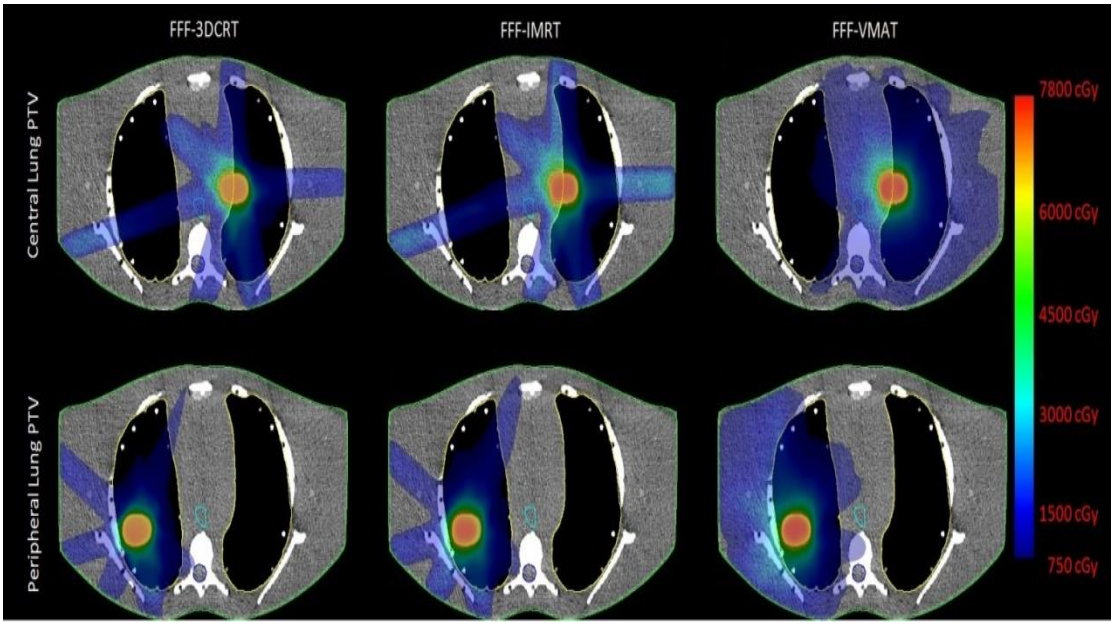

Figure 4.2 Dose distribution of the three different planning techniques for PTV#8 (both central and peripheral) in the axial plane.

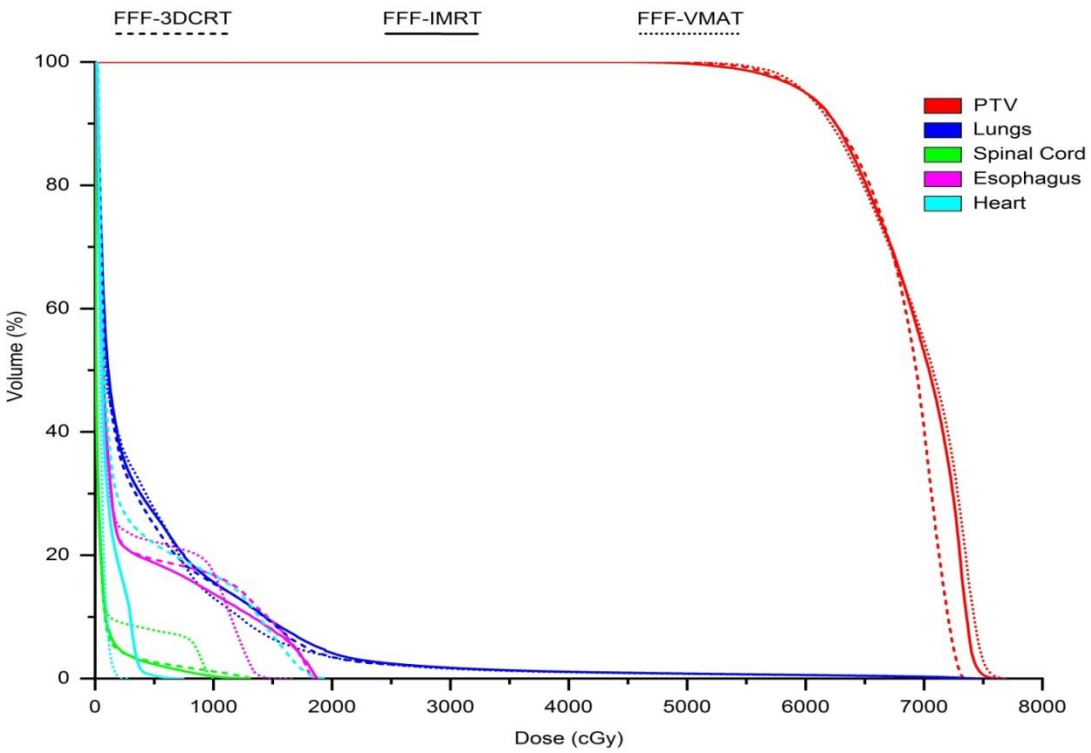

Figure 4.3 Mean dose volume histogram (DVH) of the three different planning techniques for central lung PTVs.

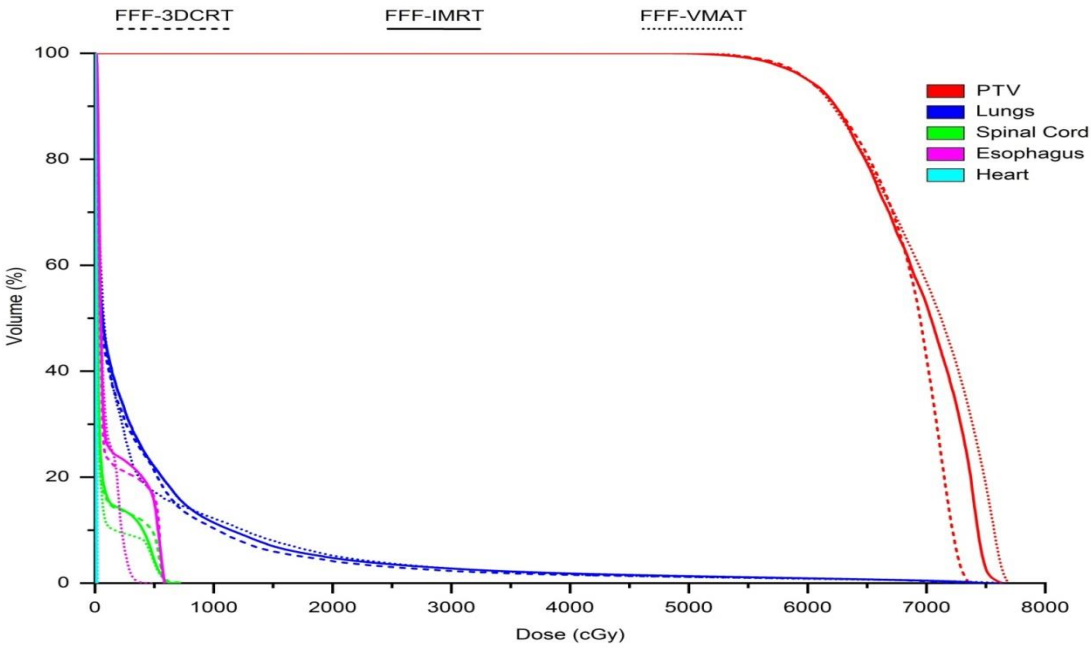

Figure 4.4 Mean dose volume histogram (DVH) of the three different planning techniques for peripheral lung PTVs.

Table 4.3 Summary of mean dosimetric indices for the FFF-3DCRT, FFF-IMRT, and FFF-VMAT treatment plans of combined lung PTVs.

Organ	Parameter	FFF-3DCRT	FFF-IMRT	FFF-VMAT	p-value		
					3DCRT vs IMRT	3DCRT vs VMAT	VMAT vs IMRT
PTV	CI	1.11±0.09	1.05±.06	1.03±0.05	0.000	0.000	0.000
	HDV (%)	1.27±0.57	0.36±0.12	0.17±0.10	0.000	0.000	0.000
	D_{2cm} (%)	49.51±8.18	45.78±5.42	42.37±5.83	0.000	0.000	0.006
	$R_{50\%}$	3.71±.99	4.16±1.08	4.05±0.80	0.003	0.011	0.732
	GI	3.32±0.54	3.59±0.65	3.75±0.53	0.001	0.000	0.003
	HI	0.24±0.02	0.26±0.01	0.26±0.01	0.001	0.001	0.011
	D_{max}(%)	124±2	128±1	129±1	0.000	0.000	0.000
	$D_{2\%}$(%)	122±2	125±1	127±1	0.000	0.000	0.000
	MUs	3973±452	5335±712	4719±650	0.000	0.000	0.000
	BOT (min)	2.85±0.32	3.82±0.51	3.45±0.51	0.000	0.000	0.000
	TT (min)	9.69±1.10	11.10±1.48	4.01±0.55	0.000	0.000	0.000
Lungs	V_{20} (%)	3.81±2.08	4.40±2.34	4.29±2.47	0.000	0.005	0.362
Spinal Cord	D_{max} (cGy)	10.46±3.49	9.77±3.28	8.26±2.05	0.006	0.000	0.000
Esophagus	D_{max} (cGy)	12.12±6.66	12.42±7.21	10.17±6.12	0.253	0.000	0.000
Heart	D_{max} (cGy)	10.40±9.57	4.09±3.43	2.45±1.78	0.040	0.040	0.040

FFF, flattening filter free; 3DCRT, three dimensional conformal radiotherapy; IMRT, intensity modulated radiotherapy; VMAT, volumetric modulated arc therapy; PTV, planning target volume; CI, conformity index; HDV, high dose volume; D_{2cm}, low dose location; $R_{50\%}$, low dose volume; GI, gradient index; HI, homogeneity index; D_{max}, maximum dose; $D_{2\%}$, near-maximum radiation dose; MUs, monitor units; BOT, beam on time; TT, treatment time; V_{20}, bilateral lung volume receiving 20 Gy or more

Table 4.4 Summary of mean dosimetric indices for the FFF-3DCRT, FFF-IMRT, and FFF-VMAT treatment plans by different lung locations.

Organ	Parameter	Central lung PTVs						Peripheral lung PTVs					
					p-value						p-value		
		FFF-3DCRT	FFF-IMRT	FFF-VMAT	3DCRT vs IMRT	3DCRT vs VMAT	VMAT vs IMRT	FFF-3DCRT	FFF-IMRT	FFF-VMAT	3DCRT vs IMRT	3DCRT vs VMAT	VMAT vs IMRT
PTV	CI	1.13±0.10	1.05±0.07	1.03±0.05	0.002	0.002	0.024	1.08±0.07	1.05±0.06	1.03±0.06	0.002	0.002	0.006
	HDV (%)	1.50±0.31	0.37±0.13	0.20±0.10	0.002	0.002	0.010	1.04±0.67	0.35±0.12	0.14±0.08	0.007	0.002	0.002
	D_{2cm} (%)	53.61±6.12	48.12±3.74	40.91±5.43	0.003	0.002	0.002	45.41±8.11	43.45±5.96	43.84±6.07	0.092	0.158	0.239
	$R_{50\%}$	4.13±1.03	4.15±1.14	4.02±0.70	0.486	0.863	0.964	3.29±0.79	3.76±1.04	3.86±0.89	0.002	0.002	0.417
	GI	3.60±0.50	3.66±0.62	3.89±0.50	0.427	0.003	0.007	3.04±0.44	3.52±0.69	3.61±0.54	0.002	0.002	0.134
	HI	0.24±0.02	0.25±0.01	0.25±0.01	0.158	0.117	0.530	0.24±0.01	0.26±0.00	0.27±0.00	0.002	0.002	0.002
	D_{max}(%)	124±3	128±1	129±1	0.002	0.004	0.071	124±1	127±1	128±1	0.002	0.002	0.003
	$D_{2\%}$(%)	121±2	124±1	126±1	0.002	0.002	0.002	122±1	125±1	127±1	0.002	0.002	0.002
	MUs	4337±292	5978±330	5338±179	0.002	0.002	0.002	3609.±230	4692±224	4101±124	0.002	0.002	0.002
	BOT(min)	3.11±0.21	4.28±0.24	3.89±0.14	0.002	0.002	0.002	2.59±0.16	3.36±0.16	3.02±0.10	0.002	0.002	0.002
	TT (min)	10.58±0.71	12.43±0.69	4.54±0.15	0.002	0.002	0.002	8.81±0 .56	9.76±0.47	3.49±0.11	0.008	0.002	0.002
Lungs	V_{20} (%)	3.49±1.94	4.07±2.32	3.41±1.99	0.005	0.144	0.003	4.12±2.24	4.74±2.42	5.18±2.67	0.002	0.002	0.009
Spinal Cord	D_{max} (cGy)	13.19±1.94	12.68 ±1.47	9.96±1.04	0.023	0.002	0.002	7.71±2.31	6.86±1.37	6.56±1.08	0.071	0.002	0.028
Esophagus	D_{max} (cGy)	18.48±2.05	19.07±3.40	15.86±2.92	0.308	0.002	0.002	5.75±0.20	5.78±0.91	4.48±0.38	0.433	0.002	0.004
Heart	D_{max} (cGy)	19.74±0.40	6.88±2.53	2.72±2.12	0.002	0.002	0.002	1.05±0.99	1.29±1.09	2.18±1.37	0.002	0.002	0.002

FFF, flattening filter free; 3DCRT, three dimensional conformal radiotherapy; IMRT, intensity modulated radiotherapy; VMAT, volumetric modulated arc therapy; PTV, planning target volume; CI, conformity index; HDV, high dose volume; D_{2cm}, low dose location; $R_{50\%}$, low dose volume; GI, gradient index; HI, homogeneity index; D_{max}, maximum dose; $D_{2\%}$, near-maximum radiation dose; MUs, monitor units; BOT, beam on time; TT, treatment time; V_{20}, bilateral lung volume receiving 20 Gy or more

4.3.8 AAA and Acuros XB algorithms

We also used the AAA algorithm for dose calculations, and the results of all dosimetric indices for the AAA algorithm were compared to the Acuros XB algorithm. Individual comparisons using the Wilcoxon test showed significant differences ($p < 0.05$) between the two algorithms for the most of dosimetric indices of three different techniques, except CI, $R_{50\%}$, GI, and D_{max} (esophagus) of three different techniques ($p > 0.05$), HDV of FFF-3DCRT ($p = 0.118$) and of FFF-IMRT ($p = 0.147$),V_{20} (lung) of FFF-VMAT ($p = 0.981$) and D_{max} (heart) of FFF-IMRT ($p = 0.292$) for combined lung PTVs; $R_{50\%}$ and GI of three different techniques ($p > 0.05$), CI of FFF-3DCRT ($p = 0.811$) and FFF-VMAT ($p = 0.843$), HDV of FFF-IMRT ($p = 0.234$), D_{max} (esophagus) of FFF-IMRT ($p = 0.121$) and FFF-VMAT ($p = 0.050$) for central lung PTVs; CI and D_{max} (esophagus) of three different techniques ($p > 0.05$), HDV of FFF-IMRT ($p = 0.506$),$R_{50\%}$ of FFF-3DCRT ($p = 0.317$) and FFF-IMRT ($p = 0.262$), GI of FFF-3DCRT ($p = 0.206$) and FFF-VMAT ($p = 0.867$), D_{max} (spinal cord) of FFF-IMRT ($p = 0.723$), D_{max} (heart) and D_{max} (esophagus) of both FFF-IMRT and FFF-VMAT($p > 0.05$) for peripheral lung PTVs.

4.3.8 Validation of TPS calculated and measured dose

The percentage differences between the measured dose and the dose calculated using Acuros XB (D_M), Acuros XB (D_W), and AAA in the central lung tumor were 0.8 %, 1.3 %, and 2.6 % for 3 cm × 3 cm, 0.8 %, 1.2 %, and 1.8 % for 6 cm × 6 cm, and 0.9 %, 1.2 %, and 1.4 % for 10 cm × 10 cm, respectively. Meanwhile, in the peripheral lung tumor, it was 1.2 %, 1.7 %, and 2.9% for 3 cm × 3 cm, 1.1 %, 1.5 %, and 2.0 % for 6 cm × 6 cm, and 0.9 %, 1.3 %, and 1.4 % for 10 cm × 10 cm, respectively. The results suggested that Acuros XB, compared with AAA, showed excellent agreement with the measurements.

4.4 DISCUSSION

The present study compared FFF-3DCRT, FFF-IMRT, and FFF-VMAT planning techniques for the SBRT of lung tumors. Both the FFF-VMAT and FFF-IMRT plans provided a better conformal dose of PTV than did FFF-3DCRT for peripheral and central lung PTVs. The conformity of the PTV dose in the FFF-VMAT plans was slightly improved compared to that of FFF-IMRT. Similar results were

reported in a previous study (Ong et al., 2010). The CI of the FFF-VMAT, FFF-IMRT, and FFF-3DCRT plans was within the clinically acceptable limit (CI ≤1.2) specified in the RTOG protocols, excluding minor deviations in the CI (CI ≤1.5) for the FFF-3DCRT plans for the smallest PTVs; that is, PTV#2 and PTV#1 in the central and peripheral lung PTVs, respectively. The FFF-IMRT and FFF-VMAT plans showed better CI results than did the FFF-3DCRT plans. We observed a small improvement in CI with the FFF-VMAT plans compared with that of the FFF-IMRT plans. Peripheral lung PTVs achieved an improved CI than the central lung PTVs. The CI values were comparable with those of other studies (Pokhrel et al., 2020; Ong et al., 2010; Verbakel et al., 2009; Wu et al., 2004; Lee et al., 2019).

For HDV and D_{2cm}, both FFF-VMAT and FFF-IMRT achieved better results than FFF-3DCRT. The SBRT plans using all three techniques showed lower HDV for peripheral lung tumors than for central lung tumors. D_{2cm} increased linearly with increasing PTV volumes for both 3DCRT and VMAT, while for IMRT, it increased significantly for PTV volumes up to 13.6 cc and remained almost flat above it. Both FFF-3DCRT and FFF-IMRT showed improved D_{2cm} results for peripheral lung PTVs, while VMAT showed improved results of D_{2cm} for central lung PTVs. VMAT used two full coplanar arcs for central lung PTVs compared with two ipsilateral arcs for peripheral lung PTVs, which may be the reason behind the improved results of D_{2cm} for central PTVs. Compared with FFF-3DCRT, both FFF-IMRT and FFF-VMAT showed improved D_{2cm} results for central and peripheral lung PTVs. The best D_{2cm} was obtained with FFF-VMAT for central lung PTVs, while FFF-IMRT showed similar D_{2cm} results for peripheral lung PTVs compared to FFF-VMAT. These results are in agreement with those of previous studies on lung SBRT (Balagamwala et al., 2012; Kannarunimit et al., 2015; Benedict et al., 2010; Holt et al., 2011).

The $R_{50\%}$ and GI values of the FFF-3DCRT plans achieved a tighter dose distribution than did the FFF-VMAT and FFF-IMRT plans. The $R_{50\%}$ values of the FFF-3DCRT plans were significantly lower than those of the other two techniques for peripheral lung PTVs, while the $R_{50\%}$ between FFF-IMRT and FFF-VMAT plans did not show significant differences. Similarly, a significant difference in $R_{50\%}$ could not be established between different planning techniques for the central lung PTVs. The mean GI values of the FFF-3DCRT and FFF-IMRT plans were lower than those of the FFF-VMAT plans, showing a better dose fall-off in normal tissue. This was

expected, as non-coplanar 3DCRT and non-coplanar IMRT reduces the beam overlap away from the tumor, which is not the case with coplanar VMAT techniques. These results are in agreement with previously reported data (Paddick et al., 2006; Hoffman et al., 2019; Wu et al., 2009; Purdie et al., 2007).

The HI, D_{max} and $D_{2\%}$ of the FFF-VMAT and FFF-IMRT plans achieved a higher value than did the FFF-3DCRT. We observed a slight improvement in HI, D_{max} and $D_{2\%}$ with the FFF-VMAT plans compared with that of the FFF-IMRT plans, except for the central lung PTVs, which showed similar HI values in the FFF-IMRT and FFF-VMAT plans. An increase in dose heterogeneity within the PTV volume may lead to further dose fall-off in normal tissues (Hong et al., 2010). Earlier studies have reported that a higher HI is associated with a lower GI (Balagamwala et al., 2012; Kannarunimit et al., 2015). HI appears to be a good indicator of plan quality, but previous SBRT literature does not seem to have made any recommendation on the optimal HI value for the PTV dose (Paddick et al., 2006; Benedict et al., 2010). Therefore, at present, the HI parameter appears to have limited utility in the optimization process of a lung SBRT plan, while the analysis of the DVHs and the dose distribution in the CT sections remains an integral part of the plan evaluation.

FFF-VMAT provided clear dose-sparing advantages to OARs among all treatment planning techniques, except for the V_{20} of the lung dose being significantly lower for the FFF-3DCRT plans due to the non-coplanar beam arrangement. The higher lung dose with FFF-VMAT was due to the volumetric distribution of the dose in the PTV by the arcs of rotation. However, the OAR doses evaluated with each treatment technique were well below the clinically acceptable levels. FFF-IMRT provided mostly better results than did the FFF-3DRT. The performance of OARs was also examined individually for the central and peripheral lung PTVs. Once again, out of all of the techniques, VMAT provided superior results. It was also observed that for peripheral tumors, FFF-3DCRT was able to offer some improvements over FFF-IMRT. However, no single location was superior for all OARs for FFF-3DCRT. Similar results have been reported previously (Holt et al., 2011; Wu et al., 2009).

Compared with FFF-3DCRT, MUs required for treatment delivery showed a higher value with both FFF-IMRT and FFF-VMAT, while the latter provided an improvement over the former. We found that despite the requirement for more MUs in FFF-VMAT plans, treatment times were shorter than those for FFF-3DCRT. The

dose rate for FFF beams can be two to four times higher than that of conventional FF beams; therefore, FFF-3DCRT has shown a slightly shorter treatment time than did FFF-IMRT. However, for FFF-VMAT plans, the treatment delivery time is largely limited by the rotational speed of the gantry and not by the dose rate. Faster delivery may further reduce the risk of intra-fractional setup errors that have been observed at treatment times greater than 15 min (Purdie et al., 2007; Otto et al., 2010; Ong et al., 2010).

TPS and photon beam dose calculation algorithms could have a major impact on dosimetric results, particularly in the case of inhomogeneous media and small field sizes. We used the Acuros XB and AAA algorithms, which are acceptable algorithms for lung RTOG protocols, for radiation dose calculation. The dosimetric indices of PTV, such as CI, HI, MU, BOT, TT, and D_{max} for Acuros XB plans, were found to be higher than those of AAA plans, while D_{2cm} was lower. When comparing the dose distributions of the two algorithms, the results showed statistically significant differences for HI, MU, BOT, TT, D_{max}, and D_{2cm}. However, the difference in CI between the two algorithms was statistically significant only for peripheral lung tumors planned with FFF-IMRT. The treatment plans calculated using Acuros XB were found to be superior to those calculated using AAA in the lung region. These results are consistent with data reported previously (Rana 2014; Hoffmann et al., 2018; Tajaldeen et al., 2019; Shiraishi et al., 2019; Yan et al., 2017).

4.5 CONCLUSIONS

The results of this study suggest that all three treatment techniques were able to deliver conformal SBRT plans while meeting the RTOG dose constraints. On the other hand, based on the comparison of dosimetric indices, such as CI, D_{2cm}, HI, and HDV, FFF-VMAT provides a superior treatment plan to FFF-IMRT and FFF-3DCRT in the treatment of peripheral and central lung PTVs. Dosimetric indices, such as $R_{50\%}$ and GI, were improved for FFF-3DCRT compared with those of FFF-VMAT. It is also clear that despite the requirement for higher MUs in the FFF-VMAT plans compared to FFF-3DCRT, the treatment delivery time is much shorter because of the superior gantry speed of the VMAT technique. The study suggests that the treatment dose calculated using Acuros XB is more accurate than that of AAA in a heterogeneous medium, such as the lung.